Electronic structure of the $Ba_{n+1}Pb_nO_{3n+1}$ homologous series

L. F. Mattheiss
AT&T Bell Laboratories, Murray Hill, New Jersey 07974
(Received 6 December 1989)

A combination of linear augmented-plane-wave and tight-binding (TB) techniques has been applied to calculate the electronic band structures of selected members of the $Ba_{n+1}Pb_nO_{3n+1}$ homologous series. The results show that the two end members of this series, Ba_2PbO_4 ($n=1$) and $BaPbO_3$ ($n=\infty$), exhibit semiconducting and metallic properties, respectively. The calculated (~ 1.7 eV) semiconductor gap in Ba_2PbO_4, which has the K_2NiF_4-type structure, is due to nearest-neighbor ($sp\sigma$) interactions between Pb(6*s*) and O(2*p*) orbitals at the apical sites. TB calculations for intermediate members of this series show that this gap vanishes for the $n=3$ phase, $Ba_4Pb_3O_{10}$, yielding semimetallic behavior. A detailed analysis of the electronic properties of this system suggests related compounds that are promising candidates for high-temperature superconductivity.

The discovery[1] of high-temperature superconductivity in the cubic $Ba_{1-x}K_xBiO_3$ system, with observed onset temperatures as high as 30 K (Ref. 2), has stimulated a continuing search for related noncuprate superconductors within the Ba-La-Pb-O (Ref. 3), Ba-Pb-Sb-O (Ref. 4), Ba-Pb-Bi-O (Refs. 5–7), and Ba-K-Pb-O (Ref. 7) families of cubic and noncubic compounds. This focus on plumbate- and bismuthate-based materials was initiated by the 1975 discovery[8] that Bi-doped $BaPb_{1-x}Bi_xO_3$ alloys superconduct in the composition range $0.05 \le x \le 0.3$, with a maximum $T_c \approx 12$ K. Except for K-doped barium bismuthate, efforts to find new materials with higher T_c's have been unsuccessful thus far, though a $T_c \approx 3.5$ K has been observed[4] in the $BaPb_{0.75}Sb_{0.25}O_3$ alloy system. Despite this limited success, it is nevertheless important to understand the basic electronic properties of these materials in order to evaluate their potential as possible high-temperature superconductors.

An interesting feature of the Ba-Pb-O system is the fact that it can be prepared with either a nearly cubic $BaPbO_3$ perovskite structure or a body-centered-tetragonal (bct) Ba_2PbO_4 layered-perovskite phase.[9] The latter compound has the same K_2NiF_4-type structure as the original cuprate high-T_c superconductor, $La_{2-x}Ba_xCuO_4$ (Ref. 10). Equally interesting is the discovery by Fu *et al.*[5] that the Ba-Pb-O and Ba-Pb-Bi-O systems form a homologous alloy series $Ba_{n+1}(Pb_{1-x}Bi_x)_nO_{3n+1}$ with bct structures that consist of n cubic-type perovskite layers ($BaPb_{1-x}Bi_xO_3$) separated by a rocksalt-type (BaO) layer. The end members of this series correspond to $Ba_2Pb_{1-x}Bi_xO_4$ ($n=1$) and $BaPb_{1-x}Bi_xO_3$ ($n=\infty$), respectively. The primitive unit cells for these end members and one intermediate ($n=2$) compound are shown in Fig. 1 for the undoped Ba-Pb-O system. Thus, in contrast to cubic $Ba_{1-x}K_xBiO_3$ (Refs. 1 and 2) and nearly cubic $BaPb_{1-x}Bi_xO_3$ (Ref. 8) and $BaPb_{1-x}Sb_xO_3$ (Ref. 4), where the superconducting carriers traverse a three-dimensional network of corner-shared PbO_6, BiO_6, or SbO_6 octahedra,[1,11,12] the present bct compounds are expected to share the two-dimensional electronic properties which are a well-known characteristic of the cuprate high-T_c superconductors.[13]

According to transport measurements on the two end-member compounds of the $Ba_{n+1}Pb_nO_{3n+1}$ homologous series, Ba_2PbO_4 ($n=1$) exhibits large-gap semiconducting behavior[7,14] whereas metallic properties are observed[15,16] for $BaPbO_3$ ($n=\infty$). An initial report[17] of superconductivity below ~ 0.4 K in $BaPbO_3$ has not been confirmed by more recent studies.[4,16] While Bi doping of the $n=\infty$ compound $BaPbO_3$ produces a $T_c \approx 12$ K superconductor,[8] no evidence for superconductivity has been observed[6,7,14] in the analogously doped $n=1$ phase, $Ba_2Pb_{1-x}Bi_xO_4$.

Two intermediate members of the $Ba_{n+1}Pb_nO_{3n+1}$ series have been identified,[5] including the $n=2$ ($Ba_3Pb_2O_7$) and $n=3$ ($Ba_4Pb_3O_{10}$) phases. In each case, it has not been possible to prepare single-phase samples. Nevertheless, transport measurements have been carried out on the latter ($n=3$) samples, which are found to con-

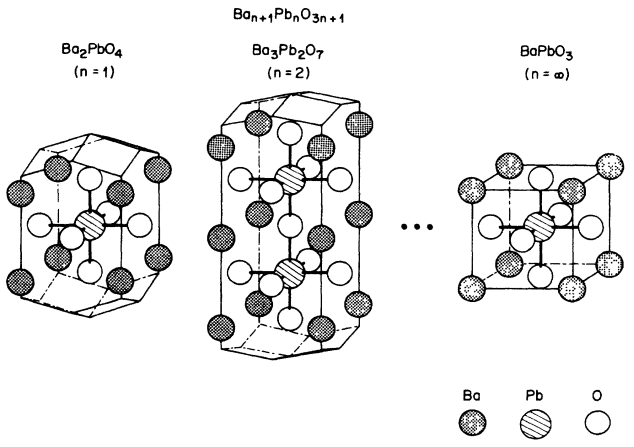

FIG. 1. Primitive unit cells for the $Ba_{n+1}Pb_nO_{3n+1}$ homologous series, including the $n=1$ (Ba_2PbO_4), $n=2$ ($Ba_3Pb_2O_7$), and $n=\infty$ ($BaPbO_3$) compounds.

sist primarily of neighboring $BaPbO_3$ and $Ba_4Pb_3O_{10}$ intergrowth regions.[5] According to these studies, the undoped materials exhibit metallic properties while the Bi-doped samples yield semiconducting behavior at low temperatures.

Without the benefit of detailed electronic-structure calculations, it is not obvious that the Ba-Pb-O system would stabilize in a series of layered perovskite-type structures with formula $Ba_{n+1}Pb_nO_{3n+1}$. In the case of La_2CuO_4, band calculations clearly show that the role of the local tetragonal Cu-O coordination geometry is to split the twofold degeneracy of the cubic e_g-type states, filling the $d(3z^2-r^2)$ sub-band and leaving the corresponding $d(x^2-y^2)$ band half filled.[13] This splitting is due to the distortion of the central CuO_6 octahedron in which two apical Cu—O bondlengths (~ 2.4 Å) are stretched relative to the planar (~ 1.9 Å) values. The result is a single half-filled band at E_F consisting of σ-antibonding Cu $d(x^2-y^2)$ and planar O $p(x,y)$ orbitals which are pointed along the Cu—O bond directions.[13]

In the case of cubic $BaPbO_3$, the chemically active Pb constituent has a partially filled 6s band, which provides neither orbital degeneracy nor anisotropy to the Pb coordination issue. In particular, calculations for cubic $BaPbO_3$ have shown[11] that the Pb(6s) band dips ~ 2 eV below the O(2p) manifold, pinning E_F near the top of the nonbonding O(2p) states (see Fig. 2). This would seem to favor an isotropic environment. In fact, structural studies[9] show that the distortion of the PbO_6 octahedron in Ba_2PbO_4 is reduced in comparison to that in La_2CuO_4. It is also opposite in sign, producing two short (~ 2.06 Å) apical Pb—O bond distances and four longer (~ 2.14 Å) planar bond lengths.

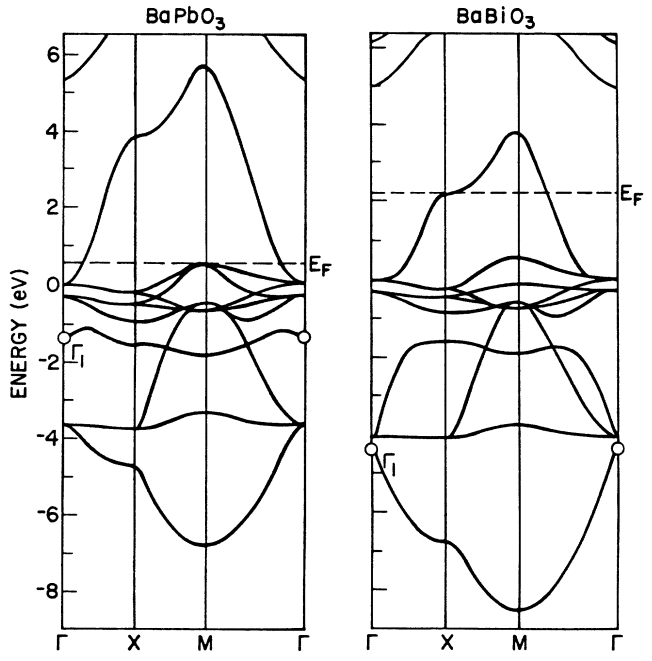

FIG. 2. LAPW energy-band results for cubic $BaPbO_3$ and $BaBiO_3$, comparing the increased binding energy of the Bi(6s) band (labeled Γ_1) relative to the corresponding Pb(6s) state.

The purpose of the present investigation is to understand the effects of this asymmetrical environment on the electronic band properties of the $Ba_{n+1}Pb_nO_{3n+1}$ series of bct compounds and to evaluate their potential as candidates for high-temperature superconductivity. This study has been carried out in two phases. The first involves the application of the linear augmented-plane-wave (LAPW) method[18] to calculate the electronic band structure of the $n=1$ phase, Ba_2PbO_4. Then, using a tight-binding (TB) model, with parameters determined by fitting the Ba_2PbO_4 LAPW results, the electronic band structures of selected intermediate phases have been calculated, including $Ba_3Pb_2O_7$ ($n=2$) and $Ba_4Pb_3O_{10}$ ($n=3$). It is found that the shortened apical Pb—O bond distance is instrumental in opening a semiconductor gap in Ba_2PbO_4, causing a single 6s-2p σ-antibonding subband to split off from the top of the nonbonding O(2p) manifold. This gap is reduced in $Ba_3Pb_2O_7$ and then vanishes for $Ba_4Pb_3O_{10}$ and the remaining members of this series.

The present LAPW calculations for Ba_2PbO_4 have been carried out self-consistently in the local-density approximation with the use of a scalar-relativistic version of the LAPW method that imposes no shape limitations on either the charge density or the potential.[18] The LAPW basis has included plane waves with energies up to 11 Ry (~ 510 LAPW's) and spherical-harmonic cutoffs of $l=8$ within the muffin-tin spheres. The charge density and potential are expanded in terms of ~ 7200 plane waves (64 Ry) in the interstitial region and by means of lattice-harmonic expansions ($l=6$) within the spheres. A twelve-point k sample in the $\frac{1}{16}$ irreducible wedge has been used to carry out the required Brillouin-zone integrations. Exchange and correlation effects are introduced via the Wigner interpolation formula.[19] The atomic Ba($5p^66s^2$), Pb($5d^{10}6s^26p^2$), and O($2s^22p^4$) states are treated as valence-band electrons in these calculations while a frozen-core approximation is applied to the deeper core levels.

The observed values[9] of the lattice and atomic position parameters for Ba_2PbO_4 are summarized in Table I. The estimated parameters for the $n=2$ phase, $Ba_3Pb_2O_7$, are also included. These have been estimated by assuming that the Pb—O and O—O bond distances in Ba_2PbO_4 are preserved in the intermediate polytypes. A crude measure of their accuracy is provided by a second extrapolation to the $n=3$ compound, $Ba_4Pb_3O_{10}$, where the estimated c-axis lattice parameter ($c=29.8$ Å) is within the 1.4% of the observed value ($c=30.2$ Å) for this phase.[5]

For orientation purposes, it is helpful to review the calculated band results for the cubic phase, $BaPbO_3$ ($n=\infty$). The results of earlier LAPW calculations[11] for $BaPbO_3$ and $BaBiO_3$ are summarized in Fig. 2. The ten-band valence manifold consists of overlapping O(2p) and Pb-Bi (6s) states, with the bottom of the 6s band labeled Γ_1 in each case. The Fermi level, which is pinned near

TABLE I. Observed (Ref. 9) (estimated) atomic position coordinates for bct Ba_2PbO_4 ($Ba_3Pb_2O_7$) with the space group $I4/mmm$ [in units of $a=4.296$ Å and $c=13.3$ Å (21.5 Å)].

	Ba_2PbO_4					$Ba_3Pb_2O_7$			
	Type	x	y	z		Type	x	y	z
Ba	4e	0.5	0.5	0.145	Ba	2b	0.5	0.5	0.0
Pb	2a	0.0	0.0	0.000	Ba	4e	0.5	0.5	0.185
O(I)	4c	0.5	0.0	0.0	Pb	4e	0.0	0.0	0.096
O(II)	4e	0.0	0.0	0.155	O(II')	2a	0.0	0.0	0.0
					O(I)	8g	0.5	0.0	0.096
					O(II)	4e	0.0	0.0	0.191

the top of the nonbonding O(2p) bands in $BaPbO_3$, rises into the broad ($sp\sigma$) antibonding sub-band in $BaBiO_3$, where it is half filled. This is accompanied by a shift of the Bi(6s) level to an increased (~ 3 eV) binding energy. Thus, in agreement with experiment,[15,16] $BaPbO_3$ is shown to be metallic as a result of the ~ 2 eV overlap of the Pb(6s) and O(2p) bands.

As shown in Fig. 3(a), the corresponding LAPW results for bct Ba_2PbO_4 exhibit significant changes near the Fermi level. Instead of overlapping O(2p) and Pb(6s) bands, the 12 occupied valence bands are now separated by a large (~ 1.7 eV) semiconductor gap from the lowest unoccupied conduction band. Naively, one might assume that this gap is due simply to a reduced 6s binding energy in the bct phase. However, variations of the LAPW orbital content within this band, as indicated by the triangle and square symbols, suggest an alternate explanation which is quantified by the TB analysis below. Namely, the fact that states near the gap in Fig. 3(a) have predominant Pb(6s)-O(II) $p(z)$ character while those near the top of the σ-antibonding sub-band feature Pb(6s)-O(I) $p(x,y)$ orbitals serves to emphasize the hybrid origin of this band. In particular, TB analysis shows that this 1.7-eV gap originates from strong ($sp\sigma$) interactions between Pb(6s) and apical O(II) $p(z)$ orbitals while the overall conduction bandwidth is due to analogous interactions with the planar O(I) oxygens. The lower portions of the unoccupied Ba(5d) bands overlap this hybrid σ-antibonding Pb(6s)-O(2p) sub-band near X. In general, the LAPW bands for Ba_2PbO_4 exhibit two-dimensional characteristics which are comparable to those in La_2CuO_4 (Ref. 13), as indicated by reduced dispersion along the Λ line in the valence-band manifold.

In order to analyze these Ba_2PbO_4 results in more detail and to facilitate calculations for the more complex intermediate phases, a simple TB model has been applied to fit the LAPW results of Fig. 3(a) at Γ, X, Z, and the Δ-line midpoint. This TB model involves a basis of Pb(6s,6p) and O(2p) orbitals and includes nearest-neighbor Pb-O and O-O interactions, which are treated in a two-center approximation. The fitted parameters are listed in Table II, along with the corresponding values for

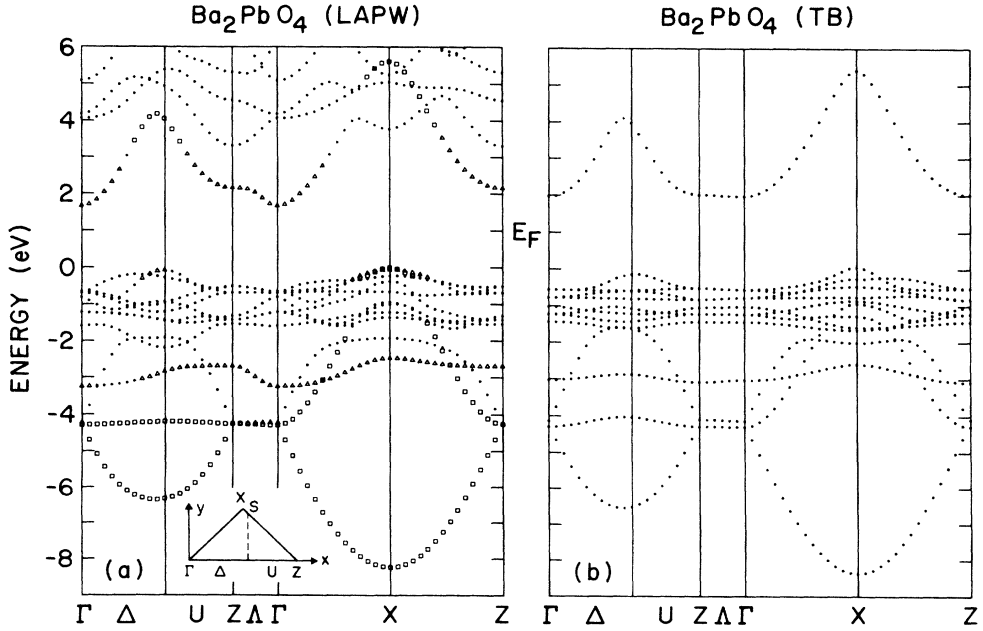

FIG. 3. Energy-band results for Ba_2PbO_4 plotted along symmetry lines of the bct Brillouin zone (see inset), as derived from (a) LAPW calculations, and (b) a tight-binding model. The triangle (square) symbols in (a) identify bands that have at least 40% Pb(6s)-O(II) $p(z)$ [Pb(6s)-O(I) $p(x,y)$] orbital weight within the corresponding muffin-tin spheres.

TABLE II. Tight-binding parameters for bct Pa_2PbO_4 and cubic $BaPbO_3$, as determined from fits to LAPW results at four symmetry points (see the text).

Ba_2PbO_4			$BaPbO_3$		
Sites [d(Å)]	Parameter	Value (eV)	Sites [d(Å)]	Parameter	Value (eV)
Pb	e_s	−1.54	Pb	e_s	−1.90
	e_p	7.0		e_p	7.0
O(I)	$e_{p\sigma}$	−0.52	O	$e_{p\sigma}$	−0.38
	$e_{p\pi}$	−1.43		$e_{p\pi}$	−1.01
O(II)	$e_{p\sigma}$	−0.59			
	$e_{p\pi}$	−0.80			
Pb-O(I)	$(sp\sigma)$	2.19	Pb-O	$(sp\sigma)$	2.25
[2.15 Å]	$(pp\sigma)$	2.90	[2.14 Å]	$(pp\sigma)$	3.02
	$(pp\pi)$	−0.39		$(pp\pi)$	−0.67
Pb-O(II)	$(sp\sigma)$	2.13			
[2.06 Å]	$(pp\sigma)$	3.11			
	$(pp\pi)$	−1.11			
O(I)-O(I)	$(pp\sigma)$	0.29	O-O	$(pp\sigma)$	0.25
[3.04 Å]	$(pp\pi)$	0.00	[3.02 Å]	$(pp\pi)$	−0.03
O(I)-O(II)	$(pp\sigma)$	0.25			
[2.98 Å]	$(pp\pi)$	−0.02			
O(II)-O(II)	$(pp\sigma)$	0.10			
[3.95 Å]	$(pp\pi)$	−0.05			
rms	error	0.22	rms	error	0.32

cubic $BaPbO_3$. As shown in Fig. 3(b), this 18-parameter TB model provides a good qualitative representation (rms error ≈ 0.2 eV) of the LAPW valence- and conduction-band results. A modified two-center treatment[20] would achieve improved accuracy within the upper valence-band energy range, but at the expense of added complexity. However, the standard two-center model is adequate for representing the essential features of the σ antibonding conduction band which play a key role in determining the electronic properties of the intermediate polytypes. The Pb($6p$) states, which lie above the energy range shown in Fig. 3(a), are essential for an accurate representation of the LAPW valence-band results, although the corresponding orbital-energy parameter is only crudely estimated.

According to the Ba_2PbO_4 TB parameters in Table II, the unhybridized Pb($6s$) level falls within the energy range of the O($2p$) complex, thereby preserving the Pb($6s$)-O($2p$) orbital degeneracy of the cubic phase in the bct compounds. A simple TB analysis shows that the LAPW gap in Ba_2PbO_4 arises from the nearest-neighbor Pb-O(II) $(sp\sigma)$ interactions. This interaction with the apical oxygens produces a pair of bonding-antibonding molecular-orbital-type states (with orbital energies $e_s = -1.54$ eV, $e_{p\sigma} = -0.59$ eV) which are then split by the off-diagonal matrix element, $\sqrt{2}(sp\sigma) \approx 3$ eV, yielding hybridized levels at $\sim +2$ and -4 eV, respectively. Similarly, the valence-conduction-band extrema at X are due to analogous planar Pb-O(I) interactions which produce an overall bandwidth of $4\sqrt{2}(sp\sigma) \approx 12.4$ eV. The combination of these interactions yields a hybrid conduction band with a net width of ~ 3.5 eV and orbital character that switches from apical to planar oxygens as one proceeds from the lower to the upper band edges.

Since both the $d(3z^2-r^2)$ and s orbitals at the Cu or Pb sites in the K_2NiF_4 structure transform according to the same point-group representation, an analogous molecular-orbital-type splitting is expected in La_2CuO_4. However, in the case of cuprates, the corresponding analysis shows[21] that the splitting $[2\sqrt{2}(pd\sigma) \approx 2.2$ eV] is reduced in magnitude to the extent that both the bonding (~ -3.7 eV) and antibonding (~ -1.5 eV) levels remain below E_F and within the valence-band energy range.

The Ba_2PbO_4 density of states (DOS) has been calculated with the use of tetrahedral interpolation involving LAPW results at 63 uniformly distributed points in the bct irreducible Brillouin-zone wedge. The calculated total and muffin-tin-projected DOS results are shown in Fig. 4. Aside from the gap, the total DOS results exhibit the same overall characteristics as the cubic compounds.[11,12] The hybrid nature of Ba_2PbO_4 conduction band is clearly reflected in the projected DOS for the planar [O(I)] and apical [O(II)] oxygens, which have increasing weight near the top and bottom of the conduction-band energy range, respectively.

Since the Pb—O and O—O bond distances have been preserved in estimating the atomic positions for the intermediate polytypes, it is straightforward to extend this TB model to these $Ba_{n+1}Pb_nO_{3n+1}$ phases. As shown in Fig. 5, this TB model yields a reduced semiconductor gap in $Ba_3Pb_2O_7$ ($n=2$) and semimetallic properties for $Ba_4Pb_3O_{10}$ ($n=3$). The $n=3$ metallic behavior is continued through the $n=\infty$ ($BaPbO_3$) polytype, as expected from a consideration of projected versions of the cubic band structure of Fig. 2.

The evolution of conduction-band states in Fig. 5 is readily understood in terms of this TB picture. The $Ba_3Pb_2O_7$ ($n=2$) phase has a central apical oxygen at the

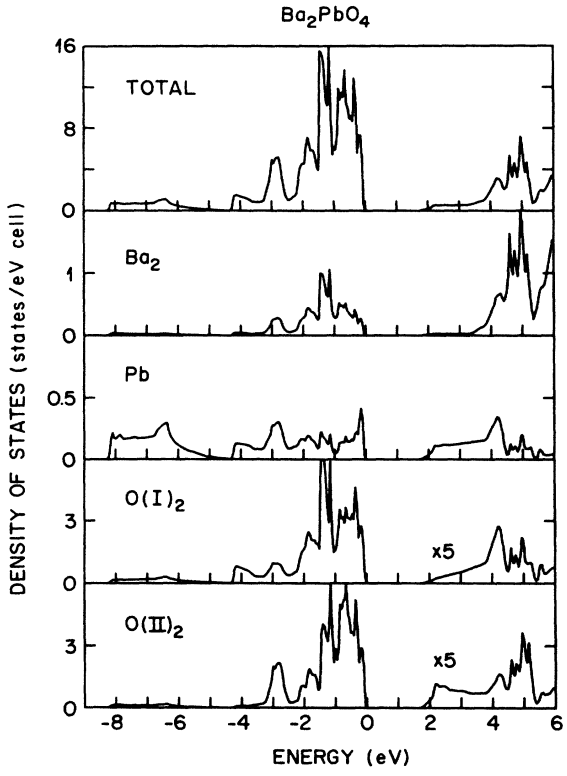

FIG. 4. Total and muffin-tin-projected density-of-states results for Ba_2PbO_4, as calculated from the LAPW bands of Fig. 3(a). Note that the projected O(I) (planar) and O(II) (apical) conduction-band results have been increased by a factor of 5 for added clarity.

origin in Fig. 1, which is labeled O(II') in Table I. The O(II') $p(z)$-type orbital is odd under reflection in the central plane, and evolves into a Γ_{2-} state[22] at the zone center. In a similar manner, the pairs of noncentral Pb($6s$) and O(II) $p(z)$ orbitals form states that are even (Γ_{1+}) and odd (Γ_{2-}) under reflection. Among the resulting antibonding conduction bands in Fig. 5(a), the energy of the upper Γ_{2-} band is increased by the interaction with two apical oxygens in comparison to the lower Γ_{1+} state, which interacts with only one. This reduced shift of the latter causes a net decrease in the band gap. A similar effect occurs in $Ba_4Pb_3O_{10}$, where the conduction band now includes two Γ_{1+} states and one with Γ_{2-} symmetry. The two Γ_{1+} states interact and produce bonding (lower) and antibonding (upper) combinations of $6s$ orbitals at neighboring c-axis Pb sites. For successive members of the $Ba_{n+1}Pb_nO_{3n+1}$ series, the lowest bonding state evolves continuously into the Γ_1 level of cubic $BaPbO_3$, which is shown in Fig. 2. Similarly, the higher-energy bands in Fig. 5 correspond to folded versions of the projected cubic bands.

While Bi doping on the Pb sublattice in the $n=\infty$ compound $BaPbO_3$ produces a $T_c \approx 12$ K (Ref. 8), superconductivity has not been observed in the tetragonal polytypes, including the $n=1$ ($Ba_2Pb_{1-x}Bi_xO_4$) (Refs. 6, 7, and 14) and $n=3$ ($Ba_4Pb_{3-x}Bi_xO_{10}$) (Ref. 5) phases. Surprisingly, transport measurements indicate that the resistivity increases with Bi doping. This suggests the possibility that chemical "order waves" on the Pb-Bi sublattice may induce semiconducting behavior, similar to that proposed[23] in $BaPb_{1-x}Bi_xO_3$ for $x \geq 0.35$. Equally interesting is the fact that K doping in $Ba_{1-x}K_xPbO_3$

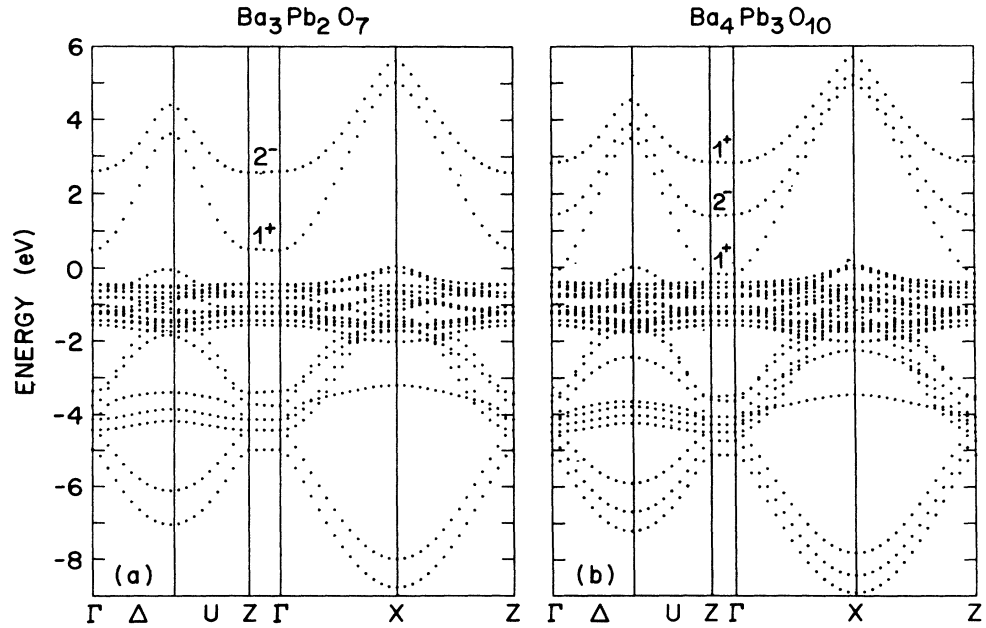

FIG. 5. Tight-binding energy-band results for (a) $Ba_3Pb_2O_7$ and (b) $Ba_4Pb_3O_{10}$.

and $Ba_{2-x}K_xPbO_4$ alloys[7] yields metallic behavior but no superconductivity. In these compounds, the Fermi level is lowered into the nonbonding O($2p$) complex, where Hirsch's mechanism[24] for hole superconductivity should be operative.

In the case of the Bi-doped materials, where electrons are added to the σ-antibonding conduction band, simple arguments based on an electron-phonon mechanism[11,12] suggest why superconductivity may be favored in the cubic $BaPb_{1-x}Bi_xO_3$ or $Ba_{1-x}K_xBiO_3$ ($n=\infty$) phases rather than the bct counterparts. In the cubic limit, model TB calculations[11] show that the maximum deformation potentials (which provide a rough measure of the electron-phonon-coupling strength) for breathing-mode displacements of the six oxygen neighbors are proportional to $\sqrt{6}\Delta(sp\sigma)$, where $\Delta(sp\sigma)$ is the change in the $(sp\sigma)$ interaction within neighboring PbO_6 or BiO_6 octahedra which alternately expand and contract. A similar analysis for the bct materials shows that the corresponding deformation potentials are reduced to $\sqrt{4}\Delta(sp\sigma)$, because of the decreased number of corner-shared oxygen [i.e., O(I)] neighbors. In both cases, these breathing-mode contributions are maximized near half filling. In the bct compounds, the corresponding contributions of the apical oxygens are concentrated near the bottom of the conduction band, thus diffusing the electron-phonon-coupling strength which is concentrated primarily at half filling in the cubic materials.

These qualitative arguments concerning the dependence of the electron-phonon-coupling strength and T_c on band filling in the cubic Ba-Pb-Bi-O and Ba-K-Bi-O phases have been confirmed by several recent calculations.[25-27] These include the tight-binding study by Shirai *et al.*[25] as well as the rigid-muffin-tin-approximation calculations by Hamada *et al.*[26] and Papaconstantopoulos *et al.*[27] In each case, it has been shown that T_c's in the 30 K range for this system can be understood in terms of the conventional electron-phonon mechanism. The extent to which this coupling is reduced in the tetragonal Ba-Pb-O phases remains an interesting question for future investigations.

However, as shown by Weber's calculations[28] for tetragonal $La_{2-x}Sr_xCuO_4$, an electron-phonon mechanism is capable of explaining T_c's in the 30–40 K range near half filling in the analogous $d(x^2-y^2)-p(x,y)$ sub-band of the cuprates. This suggests that new noncuprate high-T_c superconducting materials are possible within the bct family of $Ba_{n+1}Pb_nO_{3n+1}$ compounds. The present results suggest one particularly promising candidate, namely the oxygen-deficient $n=2$ compound, $Ba_3Pb_2O_6$. In this material, the central oxygen in Fig. 1 is removed so that each Pb now has only a single apical oxygen neighbor. This might be achieved by annealing the samples in a reducing atmosphere, or additionally, by replacing the central Ba by either Ca or Sr. The latter alternative would lead to the chemically equivalent parent compounds $Ba_2CaPb_2O_6$ or $Ba_2SrPb_2O_6$. Since each of the split conduction bands in Fig. 5(a) now interacts with a single apical oxygen, the two bands collapse to a pair of half-filled degenerate sub-bands, as shown in Fig. 6. The partial occupancy of low-lying Ba($5d$) bands [see Fig. 3(a)] would provide a possible "self-doping" mechanism. This combination of two-dimensional, half-filled, nearly degenerate sub-bands is reminiscent of the multiple-layered cuprates, where T_c tends to increase with the number of CuO_2 layers. The possibility of a similar trend in $Ba_3Pb_2O_6$ is not unreasonable.

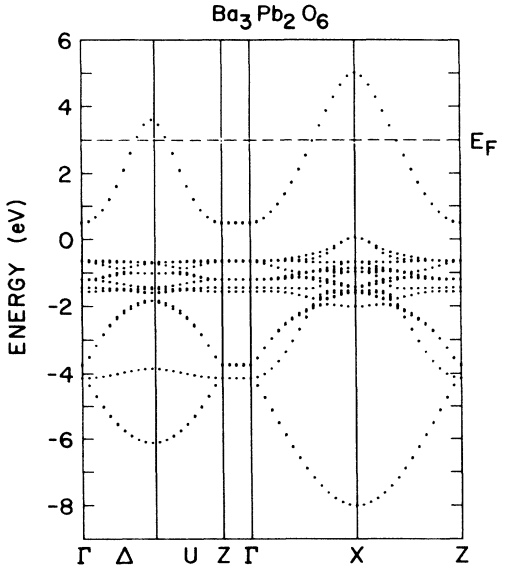

FIG. 6. Tight-binding bands for the proposed oxygen-deficient compound $Ba_3Pb_2O_6$, which contains a pair of nearly degenerate half-filled conduction bands.

In fact, two oxygen-deficient Cu-based compounds with this precise structure have been synthesized within the cuprate family.[29] These include $La_2CaCu_2O_6$ and $La_2SrCu_2O_6$, two seemingly ideal candidates for high-T_c superconductivity. However, attempts to observe this phenomenon in appropriately doped samples have been unsuccessful.[30] It has been suggested[31] that the La-Cu-O system actually forms a homologous series of $La_{n+1}Cu_nO_{3n+1}$ phases in which the formal valence of Cu, $(3-n^{-1})+$, increases systematically from 2+ (La_2CuO_4) to 3+ ($LaCuO_3$). In principle, this would allow adjustments to the valence state of Cu and possible superconductivity by means of structural variations rather than chemical doping. Unfortunately, the valence increment between the $n=1$ and $n=2$ phases skips the valence range where superconductivity is observed in the cuprates. Thus, it is not surprising that there is no empirical support for this novel idea.

It is well known[32,33] that the Sr-Ti-O system forms an analogous series of compounds with formula $Sr_{n+1}Ti_nO_{3n+1}$. However, this Ti-based series has less interesting electronic properties than its Pb or Cu counterparts since each of its member compounds is expected to exhibit semiconducting behavior. In particular, the ~3-eV band gap in nearly cubic $SrTiO_3$, which originates from the Ti($3d$)-O($2p$) orbital-energy difference,[34] should persist throughout the entire series of Sr-Ti-O bct compounds.

To summarize, the electronic properties of the $Ba_{n+1}Pb_nO_{3n+1}$ series of bct compounds have been investigated with the combined use of the LAPW and TB methods. The results show how the semiconducting gap of the $n=1$ member of this series, Ba_2PbO_4, diminishes and finally disappears for the $n=3$ compound, $Ba_4Pb_3O_{10}$, producing metallic properties for the remaining materials. The results suggest several possible noncuprate superconductors, including $Ba_3Pb_2O_6$, $Ba_2CaPb_2O_6$, and $Ba_2SrPb_2O_6$.

[1]L. F. Mattheiss, E. M. Gyorgy, and D. W. Johnson, Jr., Phys. Rev. B **37**, 3745 (1988).

[2]R. J. Cava *et al.*, Nature (London) **332**, 814 (1988).

[3]D. W. Murphy, L. F. Schneemeyer, and J. V. Waszczak, in *Chemistry of High-Temperature Superconductors II*, edited by D. L. Nelson and T. F. George (American Chemical Society, Washington, D.C., 1988).

[4]R. J. Cava *et al.*, Nature (London) **339**, 291 (1989).

[5]W. T. Fu *et al.*, Solid State Commun. **70**, 1117 (1989).

[6]K. Kourtakis and M. Robbins, Mater. Res. Bull. **24**, 1287 (1989).

[7]H. Uwe, J. Hirase, Y. Oiji, and T. Sakudo, in *Proceedings of the Tsukuba Seminar on High-T_c Superconductivity*, edited by K. Masuda, T. Arai, I. Iguchi, and R. Yoshizaki (University of Tsukuba, Tsukuba, Japan, 1989).

[8]A. W. Sleight, J. L. Gillson, and P. E. Bierstedt, Solid State Commun. **17**, 27 (1975).

[9]R. Weiss and R. Faivre, C. R. Acad. Sci. **248**, 106 (1959).

[10]J. G. Bednorz and K. A. Müller, Z. Phys. B **64**, 189 (1986); J. G. Bednorz, M. Takashigi, and K. A. Müller, Europhys. Lett. **3**, 379 (1987).

[11]L. F. Mattheiss and D. R. Hamann, Phys. Rev. B **26**, 2686 (1982); **28**, 4227 (1983).

[12]L. F. Mattheiss and D. R. Hamann, Phys. Rev. Lett. **60**, 2681 (1988).

[13]L. F. Mattheiss, Phys. Rev. Lett. **58**, 1028 (1987).

[14]Q. Xu, W. T. Fu, J. M. Ruitenbeek, and L. J. de Jongh (unpublished).

[15]R. D. Shannon and P. E. Bierstedt, J. Am. Ceram. Soc. **53**, 635 (1970).

[16]A. A. Verheijen, W. T. Fu, J. M. Ruitenbeek, A. Smits, Q. Xu, and L. J. de Jongh, Solid State Commun. **71**, 573 (1989).

[17]V. V. Bogatko and Yu. N. Venevtsev, Fiz. Tverd. Tela. (Leningrad) **22**, 1211 (1980) [Sov. Phys.—Solid State **22**, 705 (1980)].

[18]L. F. Mattheiss and D. R. Hamann, Phys. Rev. B **33**, 823 (1986).

[19]E. Wigner, Phys. Rev. **46**, 1002 (1934).

[20]L. F. Mattheiss and D. R. Hamann, Phys. Rev. B **40**, 2217 (1989).

[21]L. F. Mattheiss (unpublished).

[22]A. W. Luehrmann, Adv. Phys. **17**, 1 (1968).

[23]W. Weber, Jpn. J. Appl. Phys. **26**, Suppl. 3, 981 (1987).

[24]J. E. Hirsch and S. Tang, Solid State Commun. **69**, 987 (1989).

[25]M. Shirai, N. Suzuki, and K. Motizuki, J. Phys. Cond. Matter **1**, 2939 (1989).

[26]N. Hamada, S. Massidda, A. J. Freeman, and J. Redinger, Phys. Rev. B **40**, 4442 (1989).

[27]D. A. Papaconstantopoulos, A. Pasturel, J. P. Julien, and F. Cyrot-Lackmann, Phys. Rev. B **40**, 8844 (1989).

[28]W. Weber, Phys. Rev. Lett. **58**, 1371 (1987).

[29]N. Nguyen, C. Michel, F. Studer, and B. Raveau, Mater. Chem. **7**, 413 (1982).

[30]J. B. Torrance, Y. Yokura, A. Nazzal, and S. S. P. Parkin, Phys. Rev. Lett. **60**, 542 (1988); J. B. Torrance and R. M. Metzger, **63**, 1515 (1989).

[31]A. H. Davies and R. J. D. Tilley, Nature (London) **326**, 859 (1987).

[32]S. N. Ruddlesden and P. Popper, Acta. Crystallogr. **10**, 538 (1957); **11**, 54 (1958).

[33]R. J. D. Tilley, J. Solid State Chem. **21**, 293 (1977).

[34]L. F. Mattheiss, Phys. Rev. B **6**, 4718 (1972).

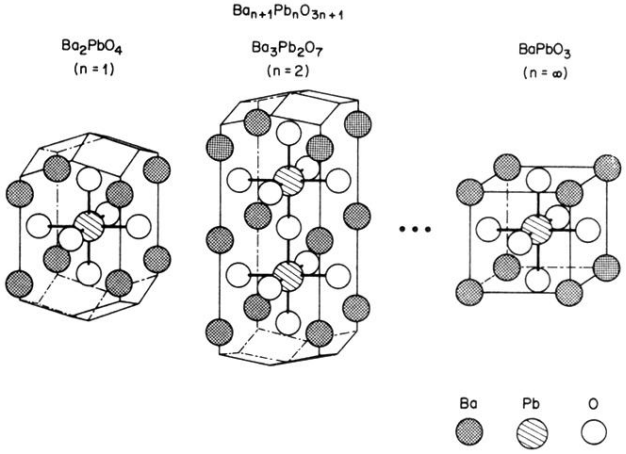

FIG. 1. Primitive unit cells for the $Ba_{n+1}Pb_nO_{3n+1}$ homologous series, including the $n=1$ (Ba_2PbO_4), $n=2$ ($Ba_3Pb_2O_7$), and $n=\infty$ ($BaPbO_3$) compounds.